

Supplemental Material and Methods

Cell Surface Downregulation of NK Cell Ligands by Patient-derived HIV-1 Vpu and Nef Alleles

Johanna Galaski, Fareed Ahmad, Nadine Tibroni, Francois M. Pujol, Birthe Müller, Reinhold E. Schmidt and Oliver T. Fackler

Cells lines and expression plasmids

HeLa TZM-bl and A3.01 T cells were cultivated in Dulbecco's modified Eagle's medium (DMEM) and RPMI 1640, respectively, supplemented with 10% fetal calf serum and 1% penicillin-streptomycin (Invitrogen). Both cell lines were obtained through the NIH AIDS Reagent Program: HeLa TZM-bl cells from Dr. John C. Kappes, Dr. Xiaoyun Wu and Tranzyme Inc. and A3.01 T cells from Dr. Thomas Folks.

The expression constructs for green fluorescent protein (GFP) fusion proteins of SF2 Nef and NL4-3 Vpu as well as for most of the corresponding mutants were described previously [1-5]. To generate Vpu H2ELV, the wild type *vpu* was PCR amplified using a 3'-end primer that contained the corresponding mutations for the acidic di-leucine motif, the product was subsequently cloned in the peGFP-N1 vector using HindIII and BamHI restriction sites [6, 7].

Isolation of genomic DNA from PBMC samples and amplification and sequencing of *vpu* and *nef* alleles

To facilitate the isolation of viral sequences also from patients with low viral load as well as the limited availability of plasma samples from these patients, proviral sequences were amplified from Peripheral blood mononuclear cells (PBMCs). PBMCs were separated using

Ficoll density gradient centrifugation. Genomic DNA was extracted from 5×10^6 PBMCs using the QIAamp DNA Blood Mini Kit (Qiagen). PCR reactions were set up according to the Q5 Hot Start High-Fidelity DNA Polymerase protocol (NEB). Primers used for the amplification of *vpu* alleles were complementary to the first exon of *tat* and the beginning of the *env* gene as described elsewhere [8] (*vpu*-forward 5846-5869 5'-CCT AGA CTA GAG CCC TGG AAG CAT-3'; *vpu*-reverse 6473-6453 5'-TTC TTG TGG GTT GGG GTC TGT-3'). Primers for the amplification of *nef* alleles were matched to regions towards the end of *env* and to the highly conserved 3' untranslated region (3'UTR) including the Poly-A signal (*nef*-forward 8685-8715 5'-GCA GTA GCT GAG GGG ACA GAT AGG GTT ATA G-3'; *nef*-reverse 9632-9607 5'-GCA CTC AAG GCA AGC TTT ATT GAG GC-3'). PCR products were gel purified using the NucleoSpin Gel and PCR Clean-up (Macherey-Nagel) and cloned into a TOPO TA cloning vector (Life Technologies). Plasmid DNA of up to ten bacterial colonies per cloning reaction was isolated using the NucleoSpin Plasmid kit (Macherey-Nagel) and were sequenced. *Nef* and *vpu* nucleotide sequences reported here were submitted to the GenBank database and have been assigned accession numbers KT698123 - KT698142 (*nef*) and KT698143 - KT698159 (*vpu*).

Phylogenetic analysis

For each patient, *vpu* and/or *nef* sequences were aligned using the ClustalW algorithm. Maximum likelihood phylogenetic trees were constructed using RaxMIGUI (by General Time Reversible (GTR) model) and edited with the software FigTree.

Cloning of selected sequences into peGFP N1 for functional analysis

A representative *vpu* or *nef* sequence was selected for every HIV-1 infected patient. *Vpu* sequences were amplified from the Topo TA constructs with specific primers containing XhoI and EcoRI restriction sites. *Nef* sequences were amplified with primers containing EcoRI and

BamHI restriction sites. *Nef* and *vpu* fragments were then subcloned into the peGFP-N1 vector.

Western blotting

For western blot analysis, HeLa TzM-bl cells were transfected with 3 μ g of expression plasmid using Lipofectamine 2000 (Life Technologies) and harvested 24 h post-transfection. Samples were boiled in sample buffer, separated by 12.5% SDS-PAGE and transferred onto a nitrocellulose membrane using a semi-dry blotting apparatus). GFP and transferrin receptor (TfR) were detected using the rat monoclonal α -GFP antibody (Chromotek) and the monoclonal mouse anti-transferrin receptor (Zymed Laboratories), respectively. For detection via the Odyssey infrared imaging system (LI-COR), membranes were incubated with IRDye 700 or 800-coupled secondary antibodies. For detection via enhanced chemiluminescence (ECL), membranes were incubated with horseradish peroxidase-coupled secondary antibodies.

Analysis of cell surface expression levels of CD4, CD317/tetherin, MHC-I, PVR, NTB-A, MICA, and ULBP-2,5,6

An initial screen of cell surface levels of relevant receptor revealed robust surface expression for most of them in HeLa TzM-bl cells. To assess cell surface levels of CD4, CD317, MHC-I, PVR and MICA, HeLa TzM-bl cells were transfected with 3 μ g of Vpu or Nef expression plasmid using Lipofectamine 2000 (Life Technologies). However, HeLa Tzm-bl cells did not express significant levels of cell surface NTB-A and ULBP-2,5,6, and effects of Vpu and Nef on these NK cell ligands were therefore assessed in A3.01 T cells, which were electroporated with 18 μ g of Vpu or Nef expression plasmid. MICB was not well expressed on any cell line available and thus not analyzed. 48 h post-transfection, cells were washed and stained in PBS with allophycocyanin (APC)-conjugated antibodies. Following antibodies were used in the

present study: APC mouse anti-human CD4 (BD Biosciences), APC mouse anti-human HLA-ABC (BD Biosciences), APC mouse anti-human CD317 (Biolegend), APC mouse anti-human CD155/PVR (R&D Systems), APC mouse anti-human NTB-A/SLAMF6 (R&D Systems), APC mouse anti-human ULBP-2,5,6 (R&D Systems), and APC mouse anti-human MICA (R&D Systems). Analysis was performed using the BD FACSVerser universal loader. 10,000 to 20,000 cells were acquired and analyzed using the FlowJo software.

Supplemental References

1. Haller C, Muller B, Fritz JV, Lamas-Murua M, Stolp B, Pujol FM, *et al.* HIV-1 Nef and Vpu are functionally redundant broad-spectrum modulators of cell surface receptors, including tetraspanins. *J Virol* 2014,**88**:14241-14257.
2. Keppler OT, Allespach I, Schuller L, Fenard D, Greene WC, Fackler OT. Rodent cells support key functions of the human immunodeficiency virus type 1 pathogenicity factor Nef. *J Virol* 2005,**79**:1655-1665.
3. Krautkramer E, Giese SI, Gasteier JE, Muranyi W, Fackler OT. Human immunodeficiency virus type 1 Nef activates p21-activated kinase via recruitment into lipid rafts. *J Virol* 2004,**78**:4085-4097.
4. Rauch S, Pulkkinen K, Saksela K, Fackler OT. Human immunodeficiency virus type 1 Nef recruits the guanine exchange factor Vav1 via an unexpected interface into plasma membrane microdomains for association with p21-activated kinase 2 activity. *J Virol* 2008,**82**:2918-2929.
5. Tervo HM, Homann S, Ambiel I, Fritz JV, Fackler OT, Keppler OT. beta-TrCP is dispensable for Vpu's ability to overcome the CD317/Tetherin-imposed restriction to HIV-1 release. *Retrovirology* 2011,**8**:9.
6. Kueck T, Neil SJ. A cytoplasmic tail determinant in HIV-1 Vpu mediates targeting of tetherin for endosomal degradation and counteracts interferon-induced restriction. *PLoS Pathog* 2012,**8**:e1002609.
7. McNatt MW, Zang T, Bieniasz PD. Vpu binds directly to tetherin and displaces it from nascent virions. *PLoS Pathog* 2013,**9**:e1003299.
8. Pickering S, Hue S, Kim EY, Reddy S, Wolinsky SM, Neil SJ. Preservation of tetherin and CD4 counter-activities in circulating Vpu alleles despite extensive sequence variation within HIV-1 infected individuals. *PLoS Pathog* 2014,**10**:e1003895.

TABLE S1. Summary of NK cell activation marker determination in the PBMCs of patients used for isolation of viral sequences.**Table S1: NK cell activation markers**

ID	NK cell activation markers (% positive NK cells)						
	CD69	DNAM-1	NKG2D	Granzyme B	Perforin	CD107a	IFN- γ
AA031	ND	ND	ND	ND	ND	ND	ND
AA002	13	55	57	76	33	29	14
UV161	22	69	52	83	53	18	6
AA041	16	66	58	71	39	42	17
AA040	17	70	68	40	35	37	10
AA032	ND	ND	ND	ND	ND	ND	ND
AA085	46	61	63	65	32	12	16
AA015	6	69	60	87	33	39	23
AA076	29	63	64	89	57	29	13
AA069	34	61	29	89	26	23	7
Jo008	23	44	33	78	29	11	6
AA068	ND	ND	ND	ND	ND	ND	ND
AA025	25	69	59	89	32	32	7
UV135	26	73	62	87	39	37	22
UV072	19	61	57	84	47	25	6
UV241	22	65	47	88	43	31	7
AA051	48	88	12	87	34	11	3
AA073	11	74	62	74	23	34	36
Jo009	25	83	68	81	22	35	14
AA017	ND	ND	ND	ND	ND	ND	ND
Jo058	ND	ND	ND	ND	ND	ND	ND
AA074	15	71	55	75	45	35	73
AA042	10	73	43	89	45	30	15
AA057	32	59	72	87	15	7	2
AA038	ND	ND	ND	ND	ND	ND	ND
UV266	9	58	59	91	35	33	10
AA052	13	64	44	58	34	41	24

TABLE S2. Summary of the number of individual viral sequences isolated per patient.**Table S2: Number of *vpu* and *nef* sequences**

Subject	<i>Vpu</i> sequences			<i>Nef</i> sequences		
	Sequence number ¹	Unique sequences ²		Sequence number ¹	Unique sequences ²	
		NT ³	AA ⁴		NT ³	AA ⁴
AA031				6	2	2
AA002	10	5	5			
UV161	6	2	1	10	7	5
AA041	7	3	3	4	1	1
AA040	2	1	1			
AA032	9	4	4			
AA085	9	6	5	10	7	7
AA015	8	7	6			
AA076	9	3	2	2	2	2
AA069				10	6	6
Jo008				9	8	7
AA068				5	2	2
AA025	6	4	4	7	2	2
UV135				10	7	6
UV072	6	1	1	10	5	4
UV241				10	5	5
AA051	7	5	5	6	2	2
AA073				7	1	1
Jo009				10	7	7
AA017				8	5	4
Jo058	10	4	3			
AA074	3	3	3	10	8	6
AA042	7	5	5	8	3	3
AA057				6	5	5
AA038	10	1	1			
UV266	7	6	6			
AA052	10	1	1	9	3	2

¹Total number of *vpu* or *nef* sequences obtained per sample

²Number of unique alleles after excluding identical sequences

³Number of unique nucleotide sequences

⁴Number of unique amino acid sequences

FIGURE S1. Vpu and Nef amino acid sequence alignment. (A) Alignment of Vpu amino acid sequences to be functionally characterized. The lab strain sequence NL4-3 Vpu serves as a reference sequence. For all other sequences, identity with the reference sequence is indicated by dots and non-conserved amino acids are specified. Dashes correspond to gaps in the alignment. Important Vpu sequence motifs are highlighted in grey boxes and labeled accordingly. (B) Alignment of Nef amino acid sequences to be functionally characterized. The lab strain sequence Nef SF2 serves as a reference sequence. For all other sequences, identity with the reference sequence is indicated by dots and non-conserved amino acids are specified. Dashes correspond to gaps in the alignment. Important Nef sequence motifs are highlighted in grey boxes and labeled accordingly.

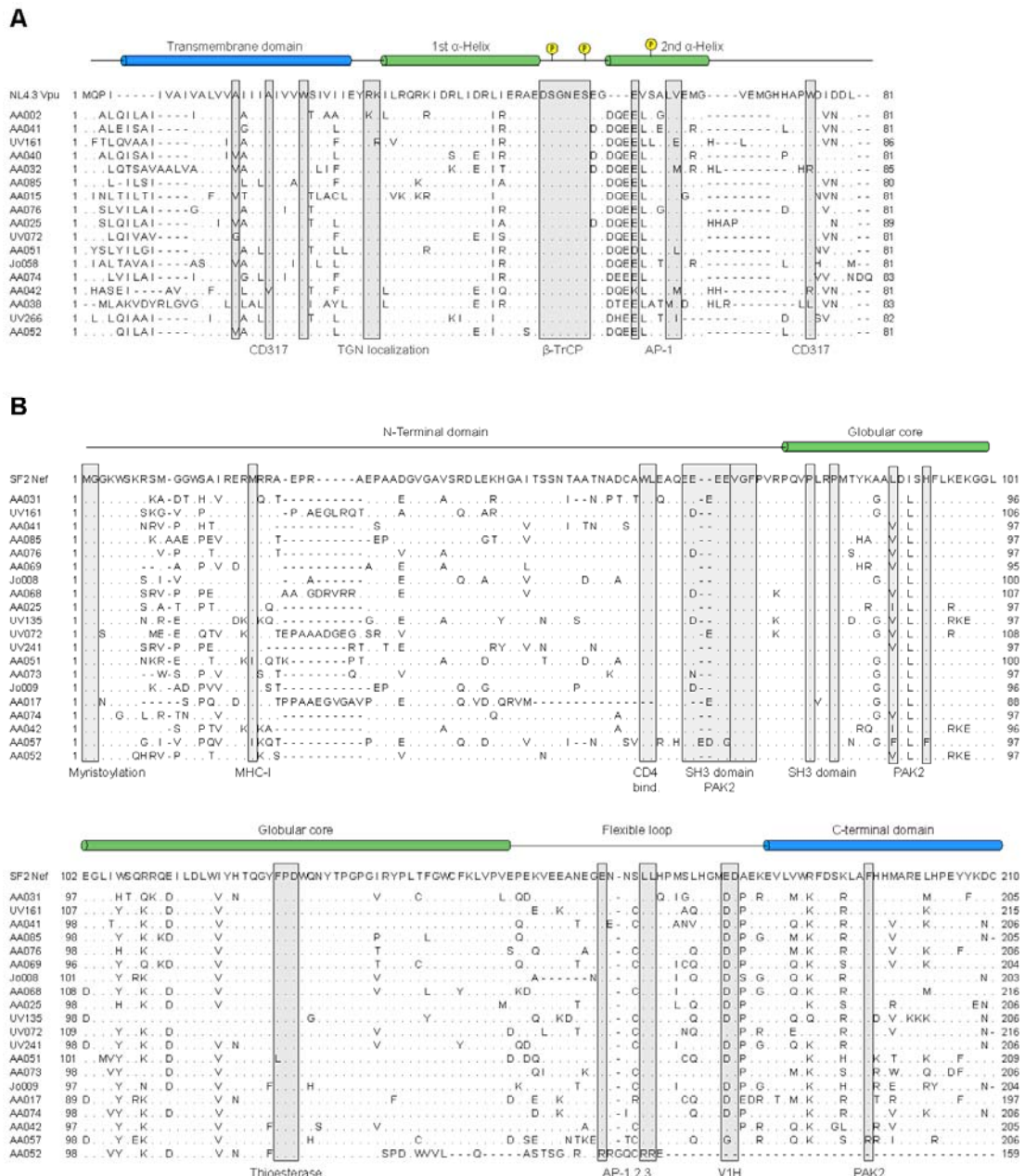


FIGURE S2. Amino acid sequence alignment of AA052 Nef sequences derived from PBMC samples collected between 2008 and 2011. The sequence of HIV-1 SF2 Nef serves as reference. Identity with the reference sequence is indicated by dots and non-conserved amino acids are specified. Dashes correspond to gaps in the alignment.

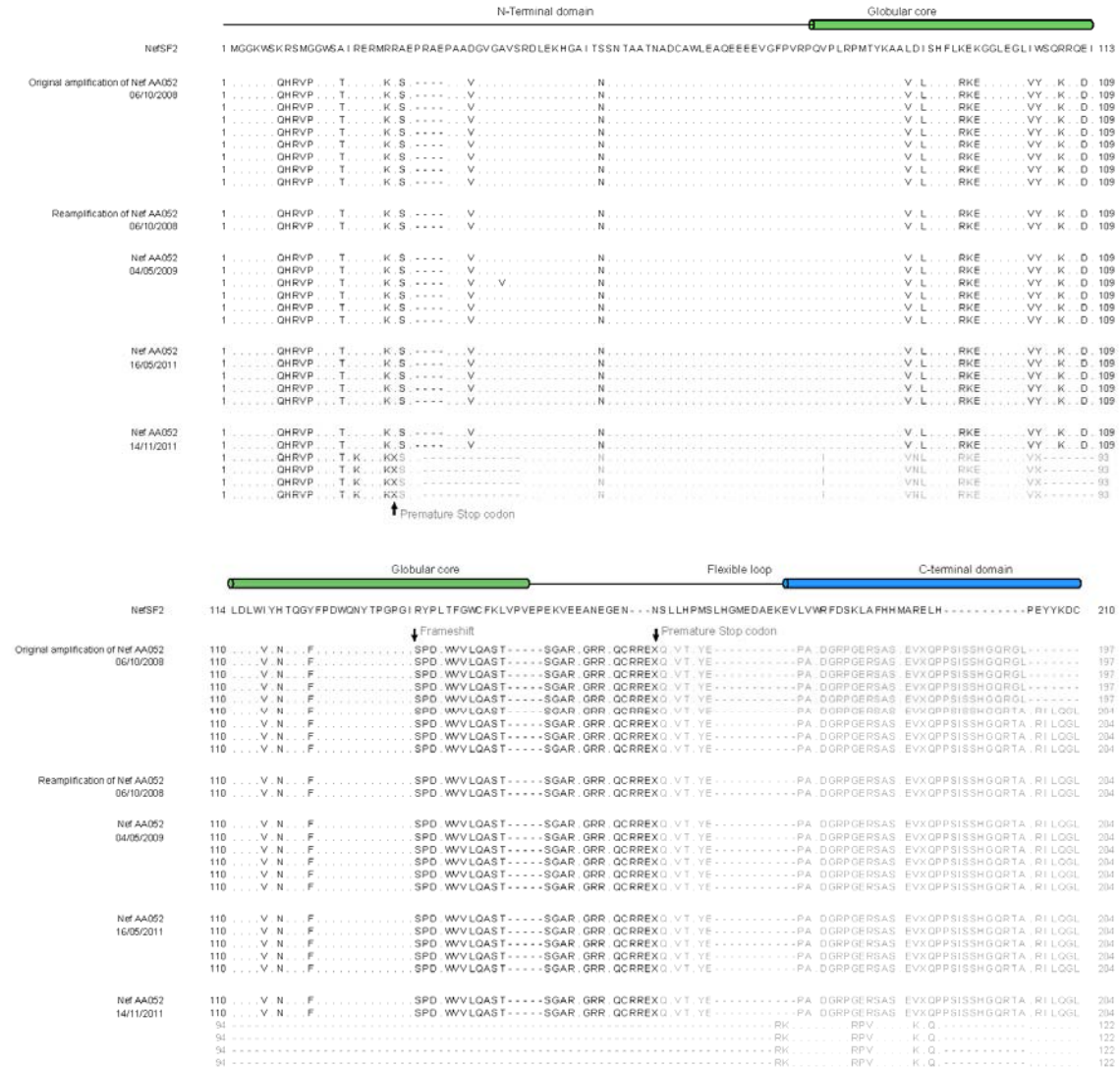


FIGURE S3. MICA downregulation by patient derived Vpu or Nef constructs. HeLa TZM-bl cells were transfected with GFP, Vpu.GFP or Nef.GFP fusion proteins. 48 hours post-transfection cell surface levels of MICA were analyzed by flow cytometry. (A) Representative flow cytometry dot plots of gated living cells transfected with GFP and NL4-3 Vpu.GFP expression plasmids are shown. The MICA.APC fluorescent intensity is displayed on the y-axis and the GFP fluorescent intensity on the x-axis. Mean fluorescent intensities are indicated. (B) The MICA surface expression relative to GFP-transfected cells is shown for all patient derived Vpu alleles. The relative surface expression for each allele was calculated by dividing the MFI of Vpu.GFP expressing cells by the MFI of Vpu.GFP negative cells. For control cells transfected with GFP this value was arbitrarily set to 100% and all other values were normalized accordingly. Stars indicate statistically significant differences to the GFP control. For clarity, only the lowest p-value that applies to all results is shown (one-way ANOVA with Dunnett's multiple comparisons test; * $p \leq 0.05$; ** $p \leq 0.01$; *** $p \leq 0.001$). Bars represent means of three independent experiments \pm SD. (C,D) As in (A,B), but for Nef fusion proteins.

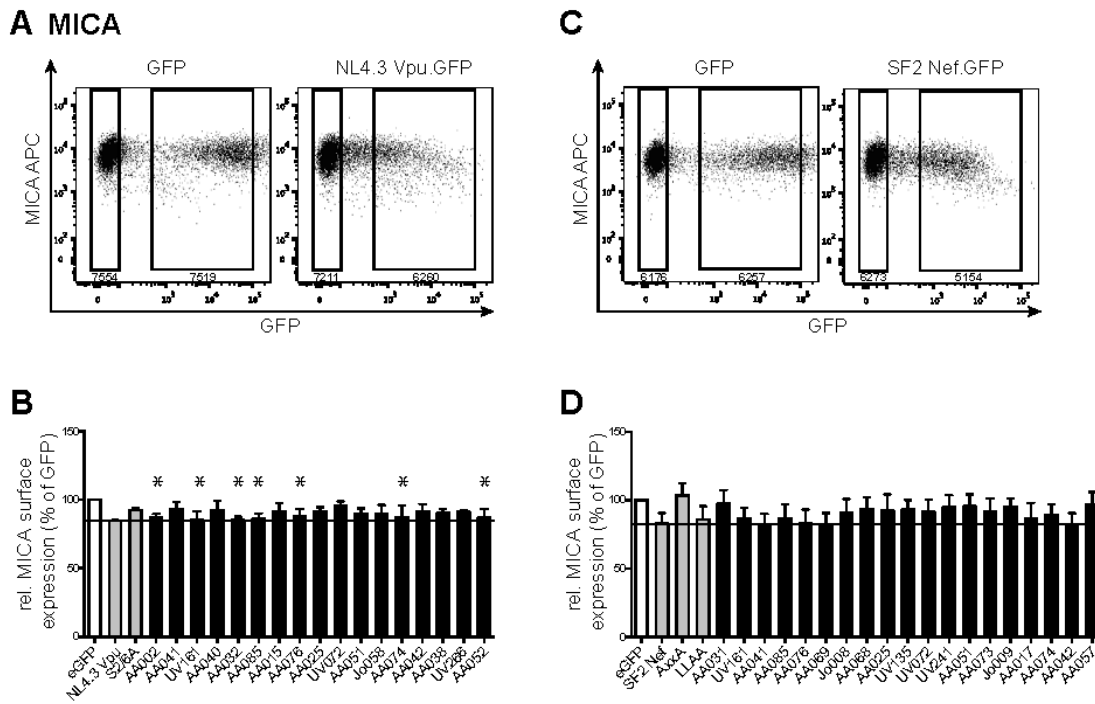


FIGURE S4. Relationship between Vpu and Nef-mediated activities and selected NK cell parameters. The patients from which *vpu* and *nef* sequences were isolated were arbitrarily stratified into cohorts with high or low NK cell count (A-C, G-I) or high or low NK cell activation (D-F, J-L). Statistical activity of NK cell ligand downregulation activity between these Vpu and Nef proteins in these two groups was assessed by Mann Whitney U-test. (A) Association between NTB-A downregulation by Vpu alleles and the patient NK cell count ($p=0.73$). (B) Association between PVR downregulation by Vpu alleles and the patient NK cell count ($p=0.41$). (C) Association between ULBP downregulation by Vpu alleles and the patient NK cell count ($p=0.73$). (D) Association between NTB-A downregulation by Vpu alleles and the percentage of CD107a positive NK cells ($p=0.98$). (E) Association between PVR downregulation by Vpu alleles and the percentage of CD107a positive NK cells ($p=0.71$). (F) Association between ULBP downregulation by Vpu alleles and the percentage of CD107a positive NK cells ($p=0.41$). (G) Association between NTB-A downregulation by Nef alleles and the patient NK cell count ($p=0.13$). (H) Association between PVR downregulation by Nef alleles and the patient NK cell count ($p=0.27$). (I) Association between ULBP downregulation by Nef alleles and the patient NK cell count ($p=0.13$). (J) Association between NTB-A downregulation by Nef alleles and the percentage of CD107a positive NK cells ($p=0.82$). (K) Association between PVR downregulation by Nef alleles and the percentage of CD107a positive NK cells ($p=0.53$). (L) Association between ULBP downregulation by Nef alleles and the percentage of CD107a positive NK cells ($p=0.63$).

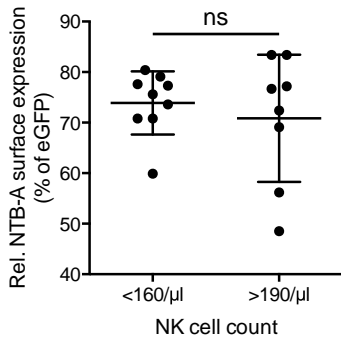
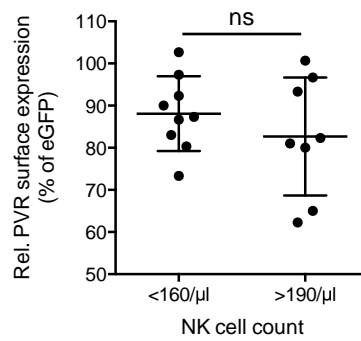
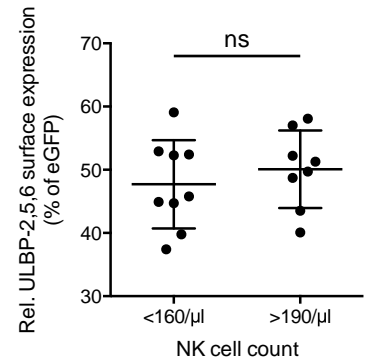
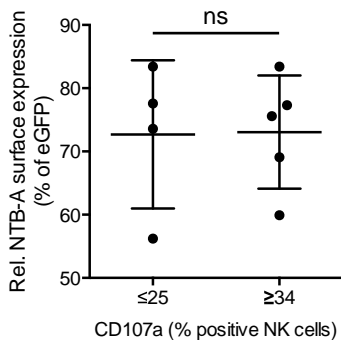
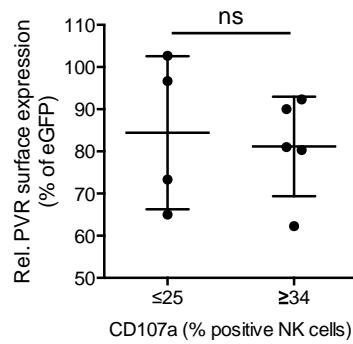
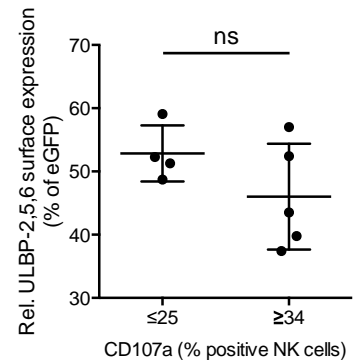
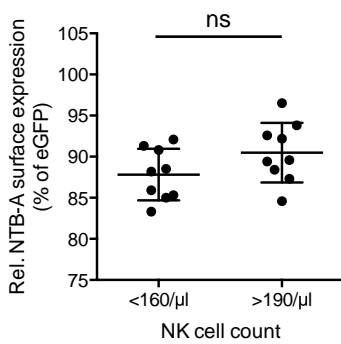
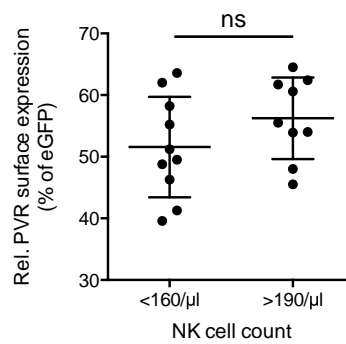
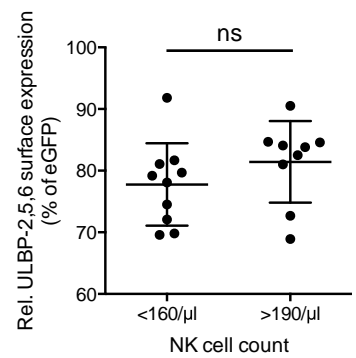
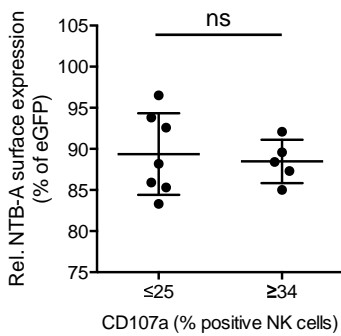
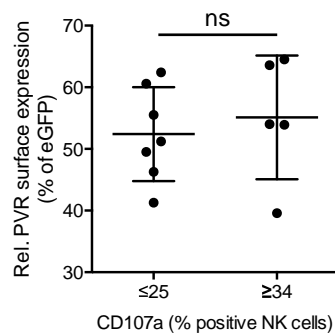
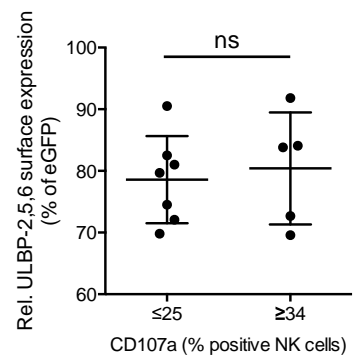
Vpu A**B****C****D****E****F****Nef G****H****I****J****K****L**

FIGURE S5. Relationship between different Vpu-mediated activities. (A-D) The correlation of PVR downregulation levels with the degree of CD4, HLA-I, CD317 and NTB-A downregulation by Vpu alleles is shown. (A) Vpu-mediated CD4 versus PVR downregulation. (B) Vpu-mediated HLA-I versus PVR. (C) Vpu-mediated CD317 versus PVR downregulation. (D) Vpu-mediated NTB-A versus PVR downregulation. (E-I) The correlation of ULBP downregulation levels with the degree of CD4, HLA-I, CD317 and NTB-A and PVR downregulation by Vpu alleles is shown. (E) Vpu-mediated CD4 versus ULBP downregulation. (F) Vpu-mediated HLA-I versus ULBP downregulation. (G) Vpu-mediated CD317 versus ULBP downregulation. (H) Vpu-mediated NTB-A versus ULBP downregulation. (I) Vpu-mediated PVR versus ULBP downregulation. Statistical analyses were done using Spearman's correlation.

Vpu

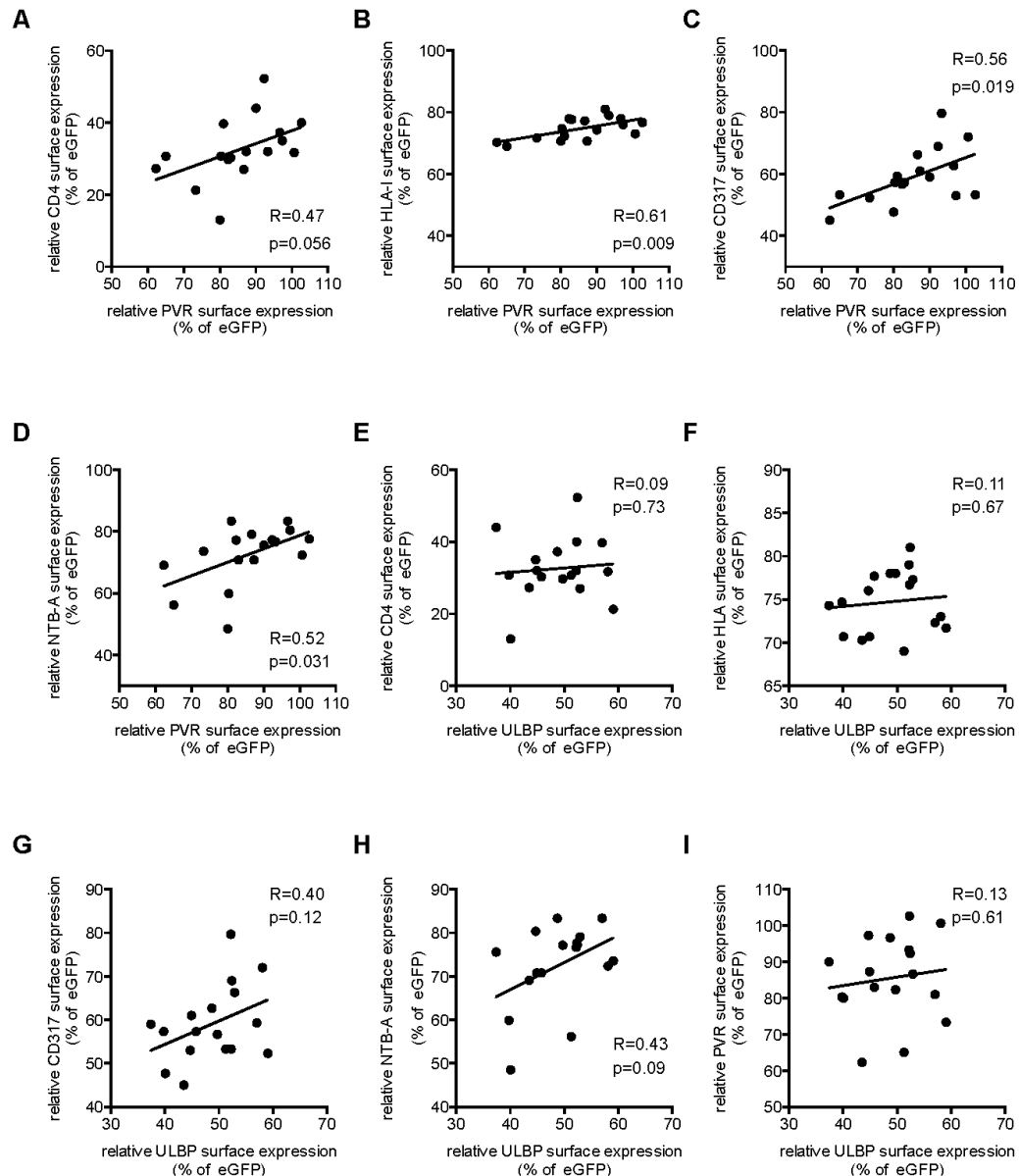


FIGURE S6. Relationship between different Nef-mediated activities. (A-D) The correlation of PVR downregulation levels with the degree of CD4, HLA-I, CD317 and NTB-A downregulation by Nef alleles with intact ORF is shown. (A) Nef-mediated CD4 versus PVR downregulation (B) Nef-mediated HLA-I versus PVR downregulation (C) Nef-mediated CD317 versus PVR downregulation. (D) Nef-mediated NTB-A versus PVR downregulation. (E-I) The correlation of ULBP downregulation levels with the degree of CD4, HLA-I, CD317 and NTB-A and PVR downregulation by Nef alleles is shown. (E) Nef-mediated CD4 versus ULBP downregulation. (F) Nef-mediated HLA-I versus ULBP downregulation. (G) Nef-mediated CD317 versus ULBP downregulation. (H) Nef-mediated NTB-A versus ULBP downregulation. (I) Nef-mediated PVR versus ULBP downregulation. Statistical analyses were done using Spearman's correlation.

Nef

